




A high-performance electrocatalyst of CoMoP@NF nanosheet arrays for hydrogen evolution in alkaline solution

Weiguo Zhang¹, Yanhui Liu¹, Haibin Zhou¹, Jun Li¹, Suwei Yao¹, and Hongzhi Wang^{1,*} 

¹Department of Applied Chemistry, School of Chemical Engineering and Technology, Tianjin University, Tianjin 300350, People's Republic of China

Received: 18 January 2019

Accepted: 21 May 2019

Published online:
28 May 2019

© Springer Science+Business
Media, LLC, part of Springer
Nature 2019

ABSTRACT

The implement of sustainable hydrogen production is a prerequisite to cater to our further energy demand. Herein, an excellent electrocatalyst of CoMoP nanosheet arrays grown on nickel foam (CoMoP NAs @NF) composite is constructed via a combination of hydrothermal and phosphating process for hydrogen evolution reaction (HER). SEM and TEM characterizations indicate the composite has a unique three-dimension structure, where CoMoP nanosheets uniformly grow on NF substrate. Due to the unique structure and the synergetic effect between CoMoP nanosheet and bare NF, electrochemical tests suggest that the composite has an excellent HER performance with a low overpotential of only 24 mV to achieve a current density of 10 mA cm⁻² and Tafel slope of 44.6 mV dec⁻¹. Moreover, a certain overpotential can be maintained at 10 mA cm⁻² for over 20 h, suggesting its superior stability. Considering its superior HER performance and stability, we envision that this composite could be a prospective substitute for non-noble-metal HER catalysts for practical applications.

Introduction

Since the increasing urgency of the environmental and energy crisis facing the world today, developing an efficient and clean new energy source to take place of the present fossil-fuel-based energy system is of great significance [1–3]. Hydrogen has been considered as a resource due to its minimal impact on the environment [4, 5]. In recent years, because of the

high product purity, merits of simple process and little pollution electrolytic hydrogen evolution reaction (HER) attracted much attention. But, the strong uphill reaction makes HER energy inefficient and costly, which is unfavorable to its practical applications [6, 7]. Although Pt and its compounds are the state-of-the-art electrocatalysts for the HER, the large-scale industrial implementation is significantly hampered by their low abundance and high cost [8, 9].

Address correspondence to E-mail: wanghz@tju.edu.cn

Therefore, it is highly imperative to develop affordable catalysts with high efficiency and stability as possible alternatives to noble metals. In fact, massive efforts focus on transition-metal-based catalysts which are proved to be catalytically active for the HER, such as transition-metal phosphides [10, 11], sulfides [12, 13], nitrides [14, 15] and carbides [16, 17]. Nevertheless, it is noted that most catalysts have better HER performance under acidic environment, while only a small part of them can express catalytic activity and stability in alkaline conditions. Given that both oxygen evolution reaction (OER) and HER are half reactions of water splitting, compatibility of them in the same electrolyte should be taken into consideration. Since most of OER catalysts are unstable in acid media, it has great industrial value to explore satisfactory HER catalysts in alkaline conditions [18, 19].

In the near future, because of their superior catalytic activity and corrosion resistance toward HER in alkaline conditions transition-metal phosphides (TMPs) have attracted great attention [20, 21]. Due to more contained electron-donating active sites and synergistic effect of different atoms, binary transition-metal phosphides usually show better HER performance than that of unary phosphides. In addition, it is an establishment that a desirable HER catalyst should have ca. zero free energy for hydrogen adsorption (ΔG_{H}) [22]. Specifically, three popular active elements for HER are included in CoMoP and it has a lower ΔG_{H} value of -0.555 eV according to DFT calculations, which is a potential HER catalyst substitute but has been rarely reported [10, 23, 24]. Despite the above mentioned, there is still plenty of room to further improve its HER performance because of its intrinsically poor electrical conductivity for CoMoP. In particular, supporting CoMoP with nickel foam (NF) is an effective approach to address this issue. For one thing, NF substrate can improve the electrical conductivity of composite; for another thing, as a three-dimension (3D) network structure, NF not only can provide a large surface area but also a free channel for electrolyte, which is beneficial to enhance the HER activity of catalysts [25]. Currently, Bai et al. [26] prepared Co/CoP-NF catalyst by a facile electrodeposition strategy, the catalyst demonstrated an excellent HER activity, it only requires 35 mV can achieve a current density of 10 mA cm^{-2} and Tafel slope of 71 mV dec^{-1} as well as good long-term durability. They attributed the excellent HER

performance to the optimized structure between bare NF and Co/CoP film. Lin et al. [27] synthesized porous CoMoP nanotubes and the catalyst displayed a high HER performance with an overpotential of 220 mV at 10 mA cm^{-2} , verifying the synergetic effect between different components in binary TMPs. Motivated by these, we fabricated the CoMoP on NF as HER electrocatalysts in alkaline solution.

In this work, we inform a facile two-step combined approach to fabricate the CoMoP nanosheets anchored on NF substrate as a valid electrocatalyst for HER in 1 M KOH. Characterizations indicate the catalyst has a unique three-dimension structure, in which CoMoP nanosheets vertically grow on NF substrate. Furthermore, electrochemical measurements indicate the catalyst possesses an outstanding HER performance with an overpotential of 24 mV at 10 mA cm^{-2} and Tafel slope of 44.6 mV dec^{-1} as well as superior stability, making it an ideal candidate for non-noble-metal HER catalysts in industrial applications.

Experimental section

Synthesis of CoMoO₄@NF

CoMoO₄@NF is prepared as follows: In a typical preparation, 1.18 g CoCl₂·6H₂O, 0.88 g (NH₄)₆Mo₇O₂₄·4H₂O and 1.2 g CO(NH₂)₂ are dissolved in 50 mL of distilled water and magnetic stirring for 30 min to form a homogeneous solution. Then, the solution is transferred into a 100 mL Teflon-lined autoclave, and a piece of NF (1 × 4 cm) is immersed in the solution. Before the immersion, the Ni foam is sonicated in 1.0 M HCl solution for 15 min to remove the superficial oxide layer and then rinsed with distilled water and absolute ethanol. Then, it is autoclaved at 120 °C for 10 h. After allowing the autoclave cooled to room temperature naturally, the CoMoO₄@NF is taken out and washed with distilled water and absolute ethanol in turn, and then dried at 60 °C overnight.

Synthesis of the CoMoP@NF electrode

The CoMoO₄@NF precursor is in center of the tube furnace, and 2.0 g of NaH₂PO₂·H₂O is placed into a separate porcelain boat on the front side of the precursor. In a nitrogen atmosphere, the temperature of

the furnace is increased to 350 °C with a ramp rate of 5 min⁻¹ and then up to 400 °C at 1 min⁻¹ and maintain it for 120 min to phosphatize the precursor. Finally, the reaction is cooled to room temperature naturally and the CoMoP@NF is achieved.

Synthesis of the CoP@NF and MoP@NF electrode

The synthesis of CoP@NF and MoP@NF electrode are prepared using the same method as CoMoP@NF electrode except without CoCl₂·6H₂O or (NH₄)₆Mo₇O₂₄·4H₂O, respectively.

Characterization

X-ray diffraction (XRD) is achieved by a Bruker D-8 ($\lambda = 1.54056 \text{ \AA}$, Cu K α radiation) with a range of 2θ from 20 to 70°. Field emission scanning electron microscopy (FESEM) (Hitachi Regulus 8200, Japan) and transmission electron microscopy (TEM) (Hitachi HT7830, Japan) are employed to study the morphology of samples. The energy-dispersive X-ray spectroscopy (EDX) is recorded by a FEI Tecnai F20 instrument at an accelerating voltage of 200 kV. X-ray photoelectron spectrometry (XPS) measurements of as-prepared samples are taken on a Perkin–Elmer PHI5300 instrument with a monochromatic Al K α as X-ray source.

For XRD and TEM characterization, CoMoO₄@NF and CoMoP@NF are scraped off from the NF substrate through continuous ultrasound in absolute ethanol solution, then collect powder by centrifugation and washed with distilled water and absolute ethanol in turn.

Electrochemical measurements

The electrochemical measurements are taken in 1 M KOH solution with electrochemical workstation (CHI660B, Inc, China), and saturated calomel electrode (SCE) electrode, graphite rod electrode and CoMoP@NF catalyst (1 × 1 cm) served as reference, counter and working electrode, respectively. In order to remove dissolved O₂, nitrogen is injected continuously for 30 min. Linear sweep voltammetry (LSV) is performed in a range from 0 to -0.2 V (vs. RHE) with a scan rate of 2 mV s⁻¹. The electrochemical impedance spectroscopy (EIS) exams are executed from 10⁵ to 10⁻¹ Hz at an overpotential $\eta = 50 \text{ mV}$

with an AC voltage of 5 mV. The stability is tested at a required constant overpotential to maintain 10 mA cm⁻² over 20 h. To assess the double-layer capacitance (C_{dl}), CV with different scan rates (10, 20, 30, 40, 50, 60 and 70 mV s⁻¹) is taken under the potential window of 0.05–0.25 V (vs. RHE). In this study, all potential values are converted to reversible hydrogen electrode (RHE) according to the equation: $E_{RHE} = E_{SCE} + 0.241 + 0.059 \text{ pH}$.

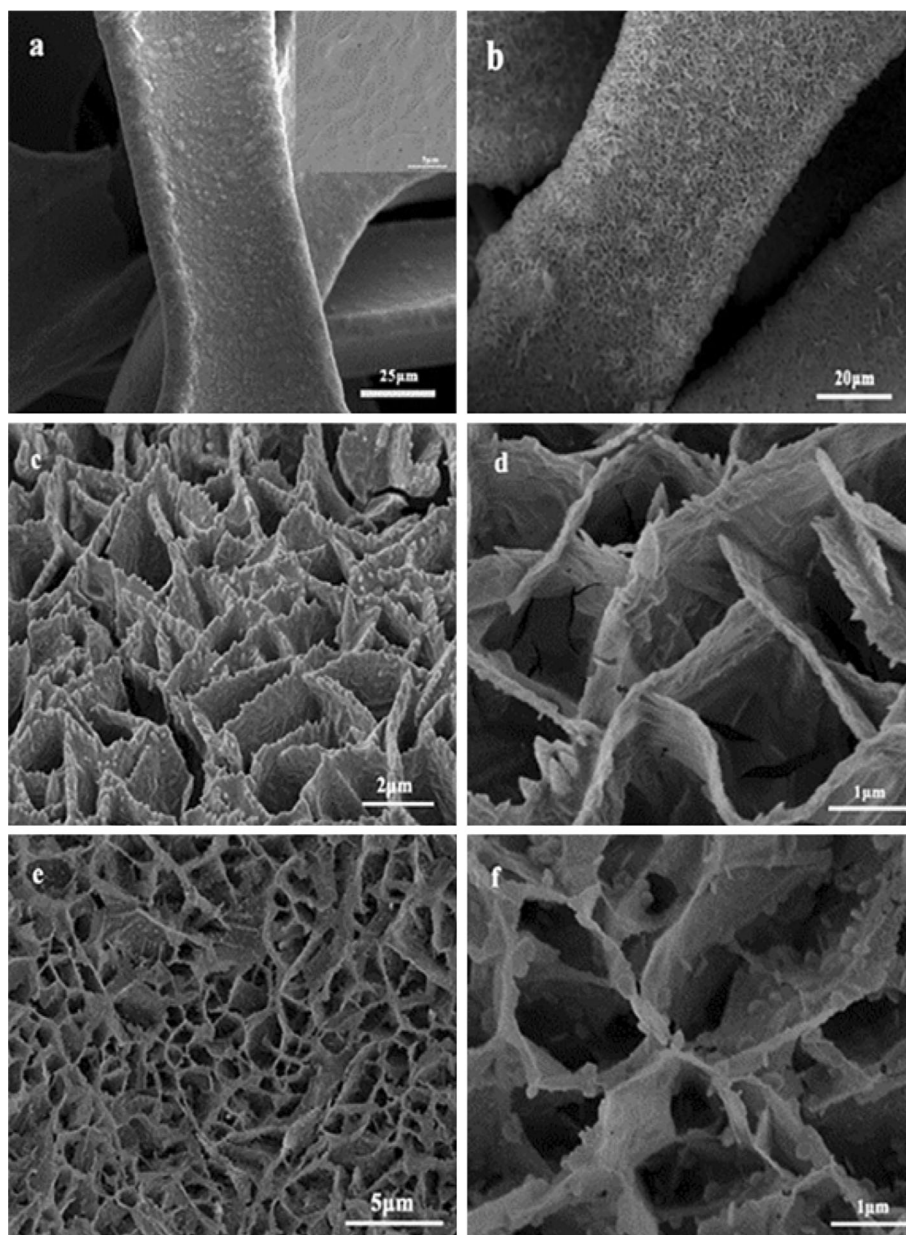
Results and discussion

Structural characterization

The morphologies of the NF, CoMoO₄@NF and CoMoP@NF catalysts are studied through scanning electron microscopy (SEM) as shown in Fig. 1. SEM examination of bare NF shows a 3D open-pore and cross-linking lattice structure with a smooth surface (Fig. 1a). After hydrothermal treatment, CoMoO₄ nanosheet arrays are well-distributed and fully covered on the NF substrate (Fig. 1b). The large-magnified SEM image exhibits that the vertically aligned CoMoO₄ nanosheet arrays form an interconnected and ordered 3D porous architectures (Fig. 1c). As shown in Fig. 1d, CoMoO₄ nanosheet arrays are relatively thin with 120 nm thickness and a smooth surface. After the phosphatization process, the morphology and structure are substantially retained. Just like CoMoO₄, the CoMoP nanosheet arrays vertically aligned on NF, interconnected with each other forming a 3D-porous architectures. As shown in Fig. 1e, the CoMoP nanosheet arrays maintain the original structure. Notably, the thickness of nanosheet arrays become thinner (about 80 nm) and numerous nanoparticles appear on the nanosheet (Fig. 1f), which are likely attributed to a complex process of decomposition on MoO_x reduction in high-temperature reduction reaction [21].

The unique structure after phosphatization possesses several advantages. Firstly, the 3D open structure formed by vertically aligned nanosheet arrays is beneficial to electrolyte and electron transportation, as well as gas evolution process [28, 29]. As known, to reach a high current density, mass transportation and fast electron are preconditions for a catalyst operation. The cooperation between CoMoP nanosheet arrays and the substrate of NF can reduce the resistance in the contact zone, so the electrons

Figure 1 SEM images of different samples. **a** Bare NF (inset: high magnification); **b** low magnification of the CoMoO₄@NF; **c, d** high magnification of the CoMoO₄@NF; **e, f** low and high magnification of CoMoP@NF.

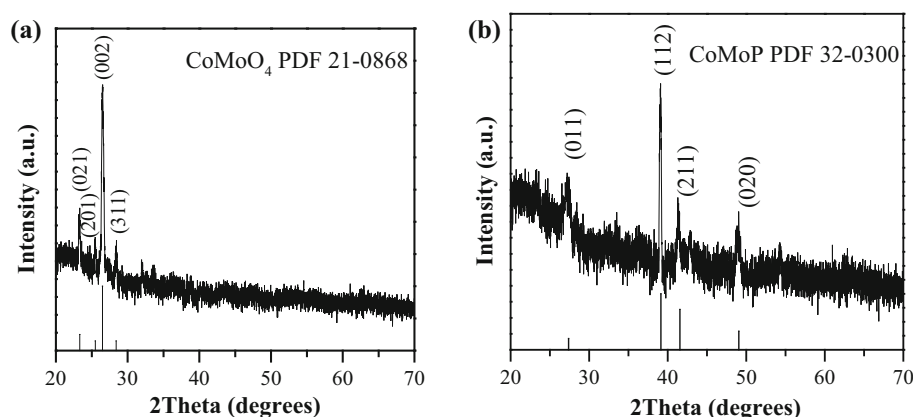


transfer between the NF substrate and the CoMoP nanosheet arrays will become easier. The rapid gas release will promote the reduce of the nanosheet–electrolyte interface region resistance, and the unique 3D open structure forming an open space among nanosheet arrays can facilitate the full use of vertical space and reveal more active sites which will benefit HER process. Secondly, compared with CoMoO₄, the CoMoP nanosheet arrays become rougher after phosphatization. A rough surface typically has more defects than smooth surface, which can be regarded

as active sites. Hence, owing to those advantages, the CoMoP@NF may display superior function in HER.

The X-ray powder diffraction (XRD) patterns are used to study the structural and crystalline information of the as-prepared samples. Because of the strong background of Ni foam, the CoMoO₄ and CoMoP have to scratch off from NF. XRD pattern of the precursor (Fig. 2a) demonstrates that the diffraction peaks are consistent with the standard patterns of CoMoO₄ phase. Four obvious and sharp diffraction peaks located at 23.3°, 25.5°, 26.5° and 28.4° can be indexed to the (021), (201), (002) and (311) planes of

Figure 2 XRD pattern **a** of the CoMoO₄ scratched off from NF; **b** of CoMoP scratch off from NF.



CoMoO₄ (JCPDS No. 21-0868), respectively. Figure 2b shows the XRD pattern of the CoMoP scratched off from NF. The diffraction peaks located at 27.3°, 39.1°, 41.5° and 49.0° are observed, which are well in line with the (011), (112), (211) and (020) planes of CoMoP (JCPDS No. 32-0300), respectively. The above results indicate that the CoMoP is successfully fabricated.

Figure 3 shows the transmission electron microscopy (TEM) images of the as-prepared CoMoP scratched off from NF. As shown in Fig. 3a, there is a nanosheet structure loaded with small nanoparticles forming a unique architecture, which is consistent with the observation on SEM results. Noticeably, those nanoparticles benefit electron transfer as well as gas release. As a consequence, such a unique architecture with high specific surface area and rich phosphorus atoms provide abundant active sites on entire surface of CoMoP nanosheet arrays. High-resolution (HR) TEM images (Fig. 3b) shows that the interplanar distance of the crystal fringes is 0.23 nm, which is corresponding to the (112) crystallographic planes of orthorhombic CoMoP (JCPDS No. 32-0300). Moreover, elemental mapping (Fig. 3e–f) results show that the surface of the area is mainly composed of Co, Mo and P elements, and those three elements are uniformly distributed and concentrated.

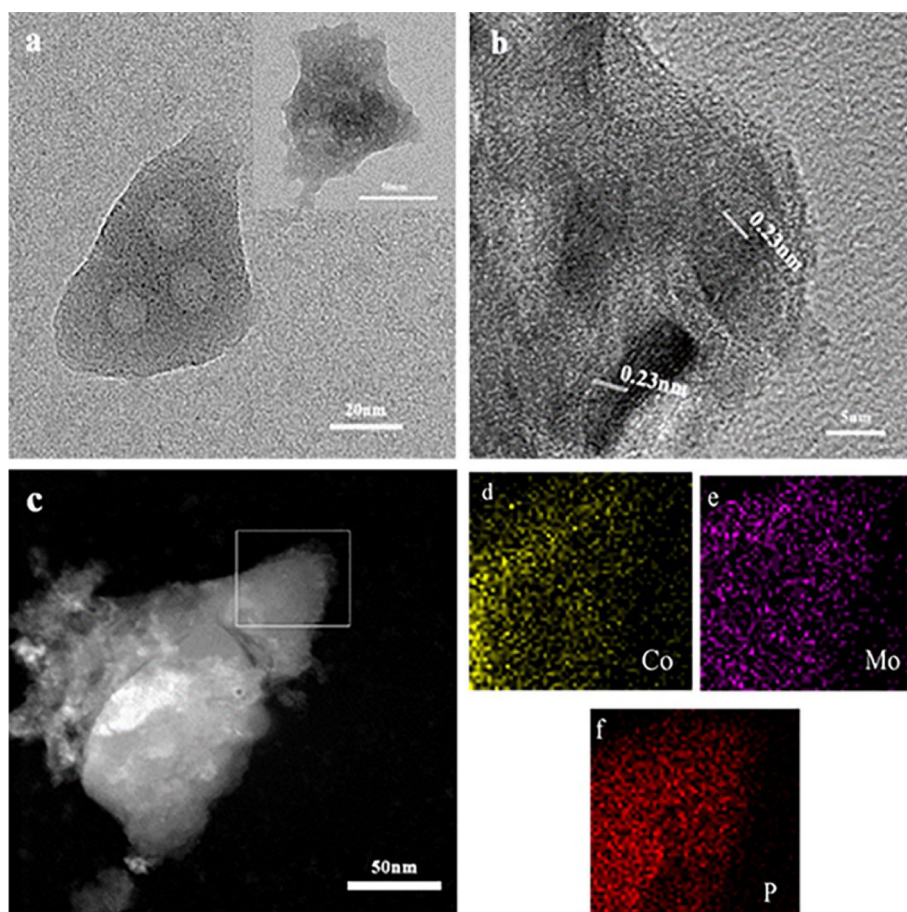
XPS tests are conducted to detect the surface chemical composition and electronic states of CoMoP@NF. The C1 s peak at 284.6 eV is corrected to all data for accuracy. As shown in Fig. 4a, the XPS survey spectrum of CoMoP@NF manifests that Co, Mo and P elements truly exist. In Fig. 4b, in the Co 2p regions, the XPS spectrum shows six distinct doublets, which show typical split-spin orbit Co 2p_{3/2} and Co 2p_{1/2} components, and the corresponding satellite peaks are accompanied. The binding

energies in Co 2p_{3/2} region at 778.2, 781.4 and 786.6 eV can be attributed to Co banded to P, oxidized Co sorts and satellite peak, respectively. In Co 2p_{1/2} region, the binding energies at 792.9, 798.4 and 802.0 eV also can be ascribed to Co banded to P, oxidized Co sorts and satellite peak [27], respectively. In Fig. 4c, the high-resolution Mo 3d spectrum of CoMoP@NF exhibits two peaks at 228.5 and 231.8 eV, which can be owing to Mo 3d_{5/2} and Mo 3d_{3/2}, respectively, and higher than the metallic Mo⁰ (227.6 eV) species, which can be ascribed to Mo^{δ+} species [30]. The peak at 230.2, 233.3, 235.5 eV can be assigned to oxidize Mo species [31]; it may be originated from the surface oxidation of CoMoP. In Fig. 4d, the P 2p of CoMoP@NF shows peaks at 129.3, 130.3 and 133.2 eV. Meanwhile, the peak at 133.2 eV can be assigned to PO₄³⁻ and the peaks at 129.3 and 130.3 eV correspond to partially negatively charged P (P^{δ-}); it can capture more positively charged protons during electrocatalytic process. Thus, results indicate that both the Co and Mo species achieve a positive charge (δ+), the corresponding P has a negative charge (δ-), indicating that the electron density will transform from Co and Mo to P. Thus, the features described above can confirm the successful preparation of CoMoP@NF.

HER activity and stability

Before measurement, the working electrode is optimized by cyclic voltammetry (CV). Figure 5a shows the linear sweep voltammetry (LSV) results at a scan rate of 2 mV s⁻¹. As a comparison, 20% commercial Pt/C, CoP@NF, CoMoO₄@NF, MoP@NF and bare NF catalyst have also been studied under the same condition. Among all materials, bare NF shows fairly

Figure 3 TEM images of samples. **a** Low and **b** high magnification images of CoMoP; **c–f** high angle annular dark field scanning transmission electron microscopy (HAADF-STEM) image and the corresponding elemental mapping images of CoMoP.



poor catalytic activity before -0.2 V. This suggests that the NF is inert against HER at a low overpotential and suitable for loading active material. The 20% commercial Pt/C catalyst exhibits outstanding activity toward HER as expected, but the HER activity of MoP@NF catalysts is not ideal because Mo has strong hydrogen adsorption free energy so the catalytic active sites are always occupied [32]. In sharp contrast, the CoMoP@NF catalysts perform a tiny onset potential of nearly zero and extremely strong cathode current. Dramatically, it only needs 24 mV and 36 mV to reach current densities of 10 and 20 mA cm⁻², respectively, which are 22 mV and 38 mV less than that of 20% commercial Pt/C. Compared with CoMoO₄@NF catalysts ($\eta_{10} = 114$ mV), CoMoP@NF catalysts imply that the introduction of phosphorus atom will greatly improve the HER. And, relative to CoP@NF catalysts ($\eta_{10} = 86$ mV), the promotional performance of CoMoP@NF catalysts can be attributed to valence state modification and synergistic effects of different components [33]. Besides, the unique 3D porous

architectures in CoMoP@NF catalysts will certainly possess a lot of active sites as well as good conductivity, which will promote the HER as well. The excellent performance is comparable to most reported values of metal phosphide electrocatalysts and most recently developed non-noble catalysts.

Tafel slope is further applied to probe the potential HER mechanism of as-prepared catalysts, which can be acquired from the curves polarization against $\log j$ by the equation of $\eta = b \log j + a$ (where b is Tafel slope, j is the current density, and a is Tafel constant). As shown in Fig. 5b, the Tafel slope of the different electrocatalysts is achieved. The Tafel slope of 50.1 mV dec⁻¹ for commercial Pt/C is agreed with the value reported in literature [34]. The higher Tafel slope can get to 128.8 mV dec⁻¹ for MoP@NF catalysts indicate its weak activity for HER. The Tafel slopes of CoMoO₄@NF catalysts and CoP@NF catalysts are 116.4 and 85.5 mV dec⁻¹, respectively. The Tafel slope of 44.6 mV dec⁻¹ of CoMoP@NF catalysts proves that it has a high active profile toward HER and this is in line with the result of the LSV test. This

Figure 4 XPS spectra of CoMoP@NF. **a** Full-scan XPS survey; high-resolution XPS signals of **b** for Co 2p; **c** for Mo; 3d; **d** for P 2p.

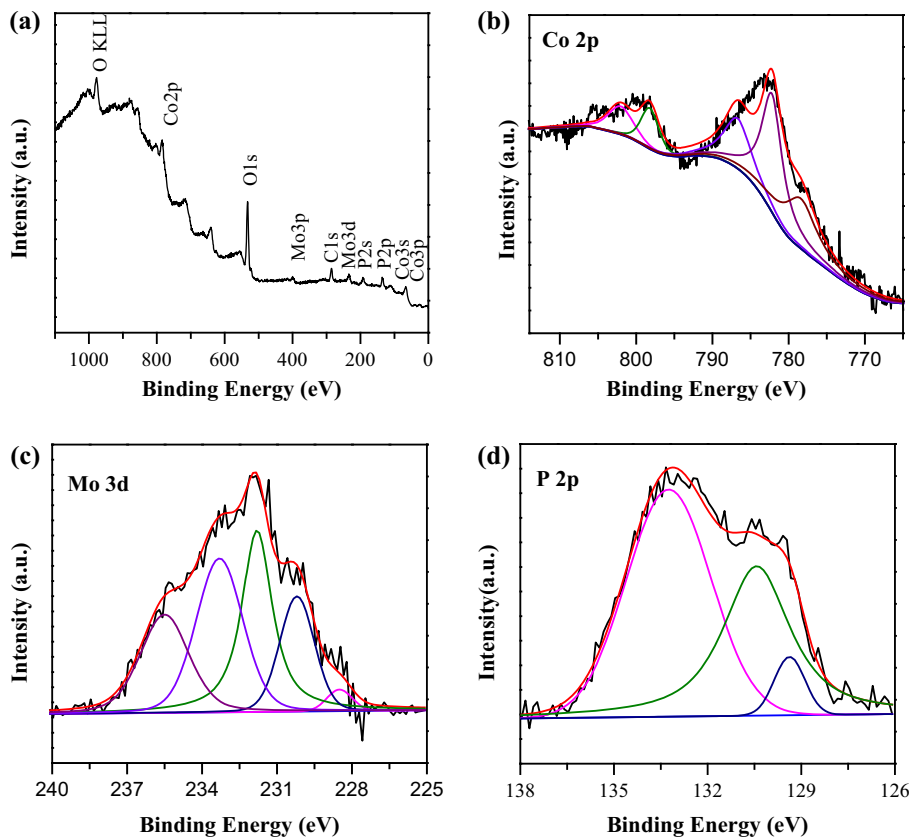
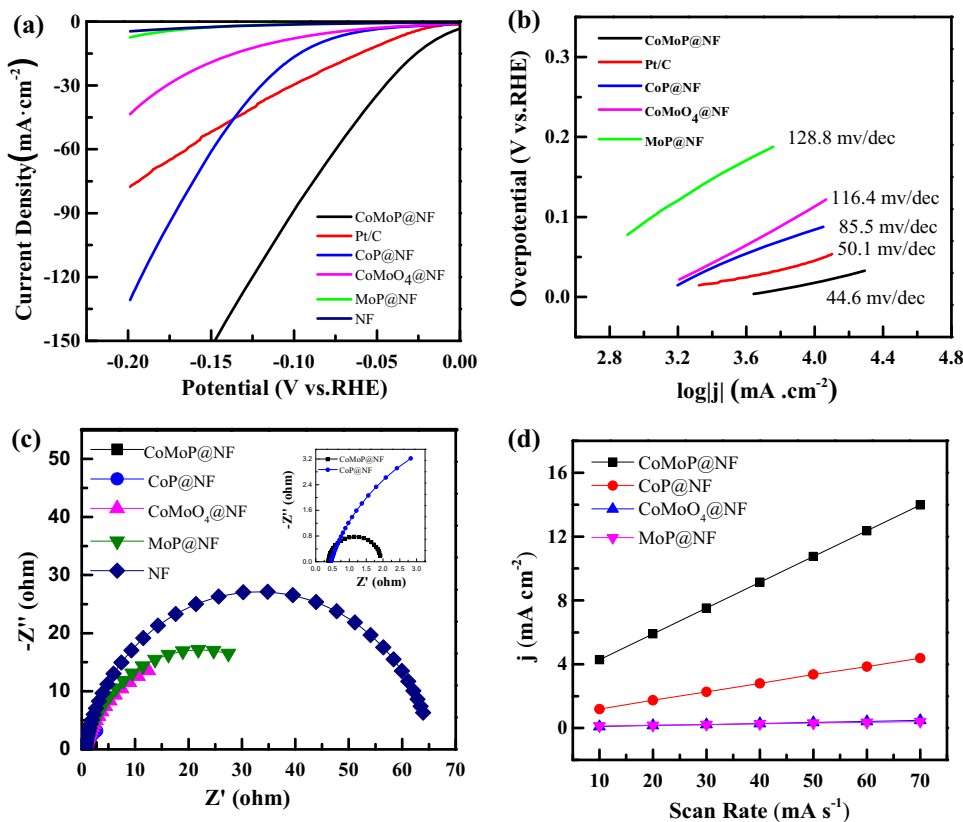


Figure 5 **a** LSV curves of CoMoP@NF, CoP@NF, CoMoO₄@NF, MoP@NF, NF and Pt/C in 1 M KOH; **b** corresponding Tafel plots; **c** corresponding AC impedance spectra at an overpotential of 50 mV (vs. HER); **d** double-layer charging currents as a function of the scan rate for different electrodes.



suggests that the HER procedure on the CoMoP@NF catalysts occurs via a typical Volmer–Heyrovsky mechanism [35]. Therefore, we can reach a conclusion: Heyrovsky step (electrochemical hydrogen desorption) with lower rates works as the rate determining step [36].

The HER catalytic activity of CoMoP@NF may be related to the unique charge properties of Co, Mo and P. As for transition-metal phosphides, it is reported that the negatively charged P can capture protons, while adsorbed H atom tends to bind to positively charged metal. The synergistic effect between transition metal and P atoms gives rise to high catalytic performance toward HER [11]. Similar to other transition-metal phosphides, CoMoP@NF has the same reaction mechanism. The negatively charged P promotes the adsorption of H^+ acting as a cationic center with strong electrostatic adsorption, and the positively charged Co, Mo attracts adsorbed H atom to form the adsorption H intermediate. In general, CoMoP@NF catalysts demonstrate excellent HER activity with a low overpotential and a small Tafel slope.

To elucidate the electrode kinetics of the catalysts during the HER process, the charge transfer kinetics are analyzed at $\eta = 50$ mV (vs. HER) using electrochemical impedance spectroscopy (EIS) in the frequency range of 100 kHz–0.01 Hz. The charge transfer resistance is determined by the diameter of semicircle at high frequencies in Nyquist plots. The Nyquist diagram of R_{ct} is related to the electrocatalytic kinetics, and a smaller value implies a faster reaction rate. As shown in Fig. 5c, in 1.0 M KOH solution, the R_s value of different catalysts is in a very narrow scope (0.4–0.7 Ω). However, the R_{ct} value is completely different. For bare NF, the R_{ct} is 86 Ω . The R_{ct} decreases to 43, 25 and 12 Ω for MoP@NF, CoMoO₄@NF and CoP@NF, respectively. In contrast, the R_{ct} of CoMoP@NF catalysts is 1.6 Ω , far lower than that of others. The small charge transfer resistance of CoMoP@NF indicates fast electron transport and enhanced conductivity. This can be attributed to the synergy between the CoMoP nanosheets and the NF substrate, which increases the electrical conductivity of the composite and accelerates the rate of electron transport in the composite. Thus, the resistance is greatly reduced, thereby increasing the activity of hydrogen evolution. The high electron transfer capacity further demonstrates the high catalytic activity of HER.

The electrochemically active surface area (ECSA) of the electrodes in 1.0 M KOH is also evaluated. According to the equation $ECSA = C_{dl}/C_s$ (where C_{dl} is electrochemical double-layer capacitance and C_s is the specific capacitance of the sample), the C_{dl} is in linear proportion to the ECSA. At a non-faradaic region (0.15 V vs. RHE in this work), the C_{dl} of catalysts can be calculated from CV tests by plotting the current density ΔJ_{ac} ($\Delta J_{ac} = J_a - J_c$, where J_a is anodic current density and J_c is cathodic current density) against the scan rates, and half of the slope is C_{dl} [37, 38]. As shown in Fig. 6a, the CoMoP@NF catalysts show the largest C_{dl} value of 162 mF cm⁻² compared to that of CoP@NF (52.6 mF cm⁻²), CoMoO₄@NF (6.3 mF cm⁻²) and MoP@NF (4.6 mF cm⁻²), indicating that CoMoP@NF catalysts expose more ECSA, and the higher ECSA means greater effective surface area and more exposed electrochemically active sites. It can be attributed to the 3D skeleton provided by the NF, which can greatly enlarge the surface area of the material, thereby increasing the contact and reaction of the electrolyte with the surface of the material, explaining its superior HER performance.

For practical application, good stability is another critical significance of HER catalysts. The chronopotentiometry test is performed to evaluate the stability of the CoMoP@NF catalysts in 1.0 M KOH. Figure 6a exhibits the changes of current density with different electrolytic time at a fixed overpotential of 24 mV. The time-dependent current density curve shows that the CoMoP@NF catalyst can maintain electrocatalytic activity for at least 20 h. In addition, it can be seen that after 5000 cycles (inset Fig. 6a), the loss of current density is negligible compared to initial curve of the LSV curve, confirming the excellent stability of the CoMoP@NF catalysts in alkaline solution, which suggests great possibilities for practical industrial applications of CoMoP@NF electrocatalysts.

Active sites (n), which is used to evaluate the intrinsic activity [8]. From CV curves (in the area of -0.05 to 0.3 V vs. RHE at the scan rate of 50 mV s⁻¹), we can calculate the n through integrating charges in 1 M KOH (Fig. 6b). If the n is calculated, the turnover frequency (TOF) can be calculated and can be used it to evaluate the intrinsic activity. At the same overpotential ($\eta = 100$ mV vs. HER), CoMoP@NF shows the largest TOF reached 0.45 s⁻¹, which is 3.01, 4.07 and 5.84 folds higher than that of CoP@NF (0.15 s⁻¹), CoMoO₄@NF (0.111 s⁻¹) and MoP@NF (0.08 s⁻¹),

Figure 6 **a** Time dependence of cathodic current density curve during electrolysis for CoMoP@NF at an overpotential of 10 mV. Inset: HER polarization curves of CoMoP@NF before and after 5000 CV cycles in 1 M KOH; **b** CVs of the different electrodes at the scan rate of 50 mV s⁻¹ in 1 M KOH.

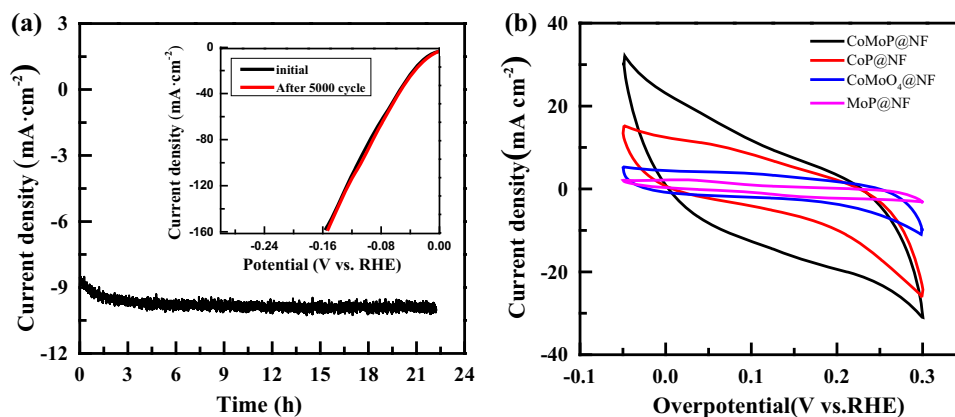


Table 1 HER parameters of various as-prepared samples

Catalyst	η_{10} (mV)	Tafel slopes (mV dec ⁻¹)	R_{ct} (Ω)	TOF (s ⁻¹ at $\eta = 100$ mV)
CoMoP@NF	24	64	1.6	0.45
CoMoO ₄ @NF	114	116.4	25	0.11
CoP@NF	86	85.5	12	0.15
MoP@NF	120	128.8	43	0.08

Table 2 Comparison of the HER performance of different electrodes

Catalysts	Electrolyte	η_{10} (mV)	Tafel plot (mV dec ⁻¹)	Refs.
CoMoP@NF	1 M KOH	24	44.1	This work
MoP@CoMoP	0.5 M H ₂ SO ₄	215	50	[24]
CoMoP@C	0.5 M H ₂ SO ₄	41	49.7	[39]
Co/CoP-NF	1 M KOH	35	71	[40]
NiCoP@NF	1 M KOH	59	39	[41]
MoP/NF	1 M KOH	114	54.6	[42]
Ni ₃ S ₂ @MoS ₂ /FeOOH	1 M KOH	189	85	[43]

respectively. It indicates that the activity of active sites in CoMoP@NF is higher (Table 1).

Based on the above results, the CoMoP@NF shows excellent HER performance and well stability. The high activity of CoMoP@NF catalyst can be attributed to its special surface composition and well-designed nanostructures: (I) The interconnected CoMoP nanosheets are uniformly and vertically grown on the NF forming a unique open-pore structure, which facilitates the rapid transport of ions in the electrolyte and vertical space can full used; (II) due to the synergistic effect among Co, Mo and P atoms (P is the negative electron center, Co and Mo is the positive charge center), as well as the valence state modification of Co and Mo, those can contribute to good electron–proton acceptability; (III) the NF can not only provide a 3D skeleton, which enlarges the surface area of the material, thereby

increasing the contact and reaction area of the electrolyte ions with the surface of the material, but also can improve the overall conductivity of the composite material which accelerates the electron transfer rate in the composite material. In summary, the as-prepared CoMoP@NF catalyst can offer a valid strategy for hydrogen production in alkaline solution (Table 2).

Conclusions

In our work, we successfully develop low-cost, stable and high active CoMoP@NF catalysts as highly efficient catalytic for HER via a two-step means of hydrothermal and phosphatization. The nanosheets grow uniformly and vertically on surface of the NF forming a 3D open pores structure. Its unique

structure exposes a great number of active sites providing excellent conductivity. Because of the close contact and synergy between CoMoP and NF, electrochemical measurements ascertain that the CoMoP@NF catalysts exhibit excellent HER activity with a low overpotential of 24 mV (vs. RHE) at 10 mA cm⁻² and a smaller Tafel slope of 44.6 mV dec⁻¹ indicates excellent electrocatalytic activity for HER, even superior to 20% commercial Pt/C in alkaline solution. In addition, stability tests suggest that the as-prepared samples show excellent durability in 1 M KOH. This work will provide an alternative pathway for essential HER catalyst design and potential practical applications in hydrogen production.

Compliance with ethical standards

Conflict of interest The authors declare that they have no conflict of interest.

References

- Jin S, May KJ et al (2011) A perovskite oxide optimized for oxygen evolution catalysis from molecular orbital principles. *Science* 334(6061):1383–1385
- Chu S, Majumdar A (2012) Opportunities and challenges for a sustainable energy future. *Nature* 488:294–303
- Hang L, Zhang T, Sun Y et al (2018) Ni_{0.33}Co_{0.67}MoS₄ nanosheets as a bifunctional electrolytic water catalyst for overall water splitting. *J Mater Chem A* 6:19555–19562
- Li J, Yan M, Zhou X et al (2016) Mechanistic insights on ternary Ni₂ - xCo_xP for hydrogen evolution and their hybrids with graphene as highly efficient and robust catalysts for overall water splitting. *Adv Funct Mater* 26:6785–6796
- Turner John A (2004) Sustainable hydrogen production. *Science* 305(5686):972–974
- Jiang Y, Lu Y, Lin J, Wang X, Shen Z (2018) A hierarchical MoP nanoflake array supported on Ni foam: a bifunctional electrocatalyst for overall water splitting. *Small Methods* 2:1700369
- Sivanantham A, Ganesan P, Shanmugam S (2016) Hierarchical NiCo₂S₄ nanowire arrays supported on Ni foam: an efficient and durable bifunctional electrocatalyst for oxygen and hydrogen evolution reactions. *Adv Funct Mater* 26:4661–4672
- Anantharaj S, Ede SR, Sakthikumar K, Karthick K, Mishra S, Kundu S (2016) Recent trends and perspectives in electrochemical water splitting with an emphasis on sulfide, selenide, and phosphide catalysts of Fe Co, and Ni: a review. *ACS Catal* 6:8069–8097
- Li X, Hao X, Abudula A, Guan G (2016) Nanostructured catalysts for electrochemical water splitting: current state and prospects. *J Mater Chem A* 4:11973–12000
- Wen L, Sun Y, Zhang C et al (2018) Cu-doped CoP nanorod arrays: efficient and durable hydrogen evolution reaction electrocatalysts at all pH values. *ACS Appl Energy Mater* 1(8):3835–3842
- Wu C, Yang Y, Dong D, Zhang Y, Li J (2017) In situ coupling of CoP polyhedrons and carbon nanotubes as highly efficient hydrogen evolution reaction electrocatalyst. *Small* 13:1602873
- Wang H, Zhou H, Zhang W, Yao S (2018) Urea-assisted synthesis of amorphous molybdenum sulfide on P-doped carbon nanotubes for enhanced hydrogen evolution. *J Mater Sci* 53:8951–8962. <https://doi.org/10.1007/s10853-018-2226-3>
- Yu XY, Feng Y, Jeon Y, Guan B, Lou XW, Paik U (2016) Formation of Ni-Co-MoS₂ nanoboxes with enhanced electrocatalytic activity for hydrogen evolution. *Adv Mater* 28:9006–9011
- Yan H, Tian C, Wang L et al (2015) Phosphorus-modified tungsten nitride/reduced graphene oxide as a high-performance, non-noble-metal electrocatalyst for the hydrogen evolution reaction. *Angew Chem Int Ed Engl* 54:6325–6329
- Cao B, Veith GM, Neuefeind JC, Adzic RR, Khalifah PG (2013) Mixed close-packed cobalt molybdenum nitrides as non-noble metal electrocatalysts for the hydrogen evolution reaction. *J Am Chem Soc* 135:19186–19192
- Wu HB, Xia BY, Yu L, Yu XY, Lou XW (2015) Porous molybdenum carbide nano-octahedrons synthesized via confined carburization in metal-organic frameworks for efficient hydrogen production. *Nat Commun* 6:6512
- Qamar M, Adam A, Merzougui B, Helal A, Abdulhamid O, Siddiqui MN (2016) Metal-organic framework-guided growth of Mo₂C embedded in mesoporous carbon as a high-performance and stable electrocatalyst for the hydrogen evolution reaction. *J Mater Chem A* 4:16225–16232
- Landon J, Demeter E, İnoğlu N et al (2012) Spectroscopic characterization of mixed Fe–Ni oxide electrocatalysts for the oxygen evolution reaction in alkaline electrolytes. *ACS Catal* 2:1793–1801
- Zhang T, Sun Y, Hang L et al (2018) Large-scale synthesis of Co/CoOx encapsulated in nitrogen-, oxygen-, and sulfur-tridoped three-dimensional porous carbon as efficient electrocatalysts for hydrogen evolution reaction. *ACS Appl Energy Mater* 1:6250–6259

- [20] Zhu H, Gu L, Yu D et al (2017) The marriage and integration of nanostructures with different dimensions for synergistic electrocatalysis. *Energy Environ Sci* 10:321–330
- [21] Fang SL, Chou TC, Samireddi S, Chen KH, Chen LC, Chen WF (2017) Enhanced hydrogen evolution reaction on hybrids of cobalt phosphide and molybdenum phosphide. *R Soc Open Sci* 4:161016
- [22] Zheng Y, Jiao Y, Jaroniec M, Qiao SZ (2015) Advancing the electrochemistry of the hydrogen-evolution reaction through combining experiment and theory. *Angew Chem Int Ed Engl* 54:52–65
- [23] Stinner C, Prins R, Weber T (2001) Binary and ternary transition-metal phosphides as HDN catalysts. *J Catal* 202:187–194
- [24] Wang D, Zhang X, Zhang D, Shen Y, Wu Z (2016) Influence of Mo/P ratio on CoMoP nanoparticles as highly efficient HER catalysts. *Appl Catal A* 511:11–15
- [25] Guo P, Wu Y-X, Lau W-M, Liu H, Liu L-M (2017) Porous CoP nanosheet arrays grown on nickel foam as an excellent and stable catalyst for hydrogen evolution reaction. *Int J Hydrogen Energy* 42:26995–27003
- [26] Bai N, Li Q, Mao D, Li D, Dong H (2016) One-step electrodeposition of Co/CoP film on Ni foam for efficient hydrogen evolution in alkaline solution. *ACS Appl Mater Interfaces* 8:29400–29407
- [27] Lin Y, Liu M, Pan Y, Zhang J (2017) Porous Co–Mo phosphide nanotubes: an efficient electrocatalyst for hydrogen evolution. *J Mater Sci* 52:10406–10417. <https://doi.org/10.1007/s10853-017-1204-5>
- [28] Pi M, Wu T, Zhang D, Chen S, Wang S (2016) Self-supported three-dimensional mesoporous semimetallic WP_2 nanowire arrays on carbon cloth as a flexible cathode for efficient hydrogen evolution. *Nanoscale* 8:19779–19786
- [29] Sun Y, Xu K, Wei Z et al (2018) Strong electronic interaction in dual-cation-incorporated $NiSe_2$ nanosheets with lattice distortion for highly efficient overall water splitting. *Adv Mater* 30:1802121
- [30] Wang D, Zhang D, Tang C, Zhou P, Wu Z, Fang B (2016) Hydrogen evolution catalyzed by cobalt-promoted molybdenum phosphide nanoparticles. *Catal Sci Technol* 6:1952–1956
- [31] Ma RG, Zhou Y, Chen YF et al (2015) Ultrafine molybdenum carbide nanoparticles composited with carbon as a highly active hydrogen-evolution electrocatalyst. *Angew Chem Int Ed* 54:14936–14940
- [32] Cao S, Chen Y, Wang CJ, Lv XJ, Fu WF (2015) Spectacular photocatalytic hydrogen evolution using metal-phosphide/CdS hybrid catalysts under sunlight irradiation. *Chem Commun (Camb)* 51:8708–8711
- [33] Ma L, Hu Y, Chen R et al (2016) Self-assembled ultrathin $NiCo_2S_4$ nanoflakes grown on Ni foam as high-performance flexible electrodes for hydrogen evolution reaction in alkaline solution. *Nano Energy* 24:139–147
- [34] Li H, Wen P, Li Q et al (2017) Earth-abundant iron diboride (FeB_2) nanoparticles as highly active bifunctional electrocatalysts for overall water splitting. *Adv Energy Mater* 7:1700513
- [35] Conway BE, Tilak BV (2002) Interfacial processes involving electrocatalytic evolution and oxidation of H_2 , and the role of chemisorbed H. *Electrochim Acta* 47:3571–3594
- [36] Zhang J, Wang T, Liu P et al (2017) Efficient hydrogen production on $MoNi_4$ electrocatalysts with fast water dissociation kinetics. *Nat Commun* 8:15437
- [37] Chang YH, Lin CT, Chen TY et al (2013) Highly efficient electrocatalytic hydrogen production by $MoS(x)$ grown on graphene-protected 3D Ni foams. *Adv Mater* 25:756–760
- [38] Liu P, Zhu J, Zhang J et al (2017) P dopants triggered new basal plane active sites and enlarged interlayer spacing in MoS_2 nanosheets toward electrocatalytic hydrogen evolution. *ACS Energy Lett* 2:745–752
- [39] Ma YY, Wu CX, Feng XJ et al (2017) Highly efficient hydrogen evolution from seawater by a low-cost and stable $CoMoP@C$ electrocatalyst superior to Pt/C. *Energy Environ Sci* 10:788
- [40] Bai N, Li Q, Mao D, Li D, Dong H (2016) One-step electrodeposition of Co/CoP film on Ni foam for efficient hydrogen evolution in alkaline solution. *ACS Appl Mater Interfaces* 8:29400–29407
- [41] Cai Z, Wu A, Yan H et al (2018) Hierarchical whisker-on-sheet $NiCoP$ with adjustable surface structure for efficient hydrogen evolution reaction. *Nanoscale* 10:7619
- [42] Jiang Y, Lu Y, Lin J, Wang X, Shen Z (2018) A hierarchical MoP nanoflake array supported on Ni foam: a bifunctional electrocatalyst for overall water splitting. *Small Methods* 2:1700369
- [43] Zheng M, Guo K, Jiang WJ et al (2019) When MoS_2 meets $FeOOH$: a “one-stone-two-birds” heterostructure as a bifunctional electrocatalyst for efficient alkaline water splitting. *Appl Catal B* 244:1004–1012

Publisher's Note Springer Nature remains neutral with regard to jurisdictional claims in published maps and institutional affiliations.